Supplementary Materials: Comparison of scanning lidar with other remote sensing measurements and transport model predictions for a Saharan dust case

Hengheng Zhang [1]*, Frank Wagner [1,2], Harald Saathoff [1], Heike Vogel [1], Gholam Ali Hoshyaripour [1], Vanessa Bachmann [2], Jochen Förstner [2], Thomas Leisner [1]

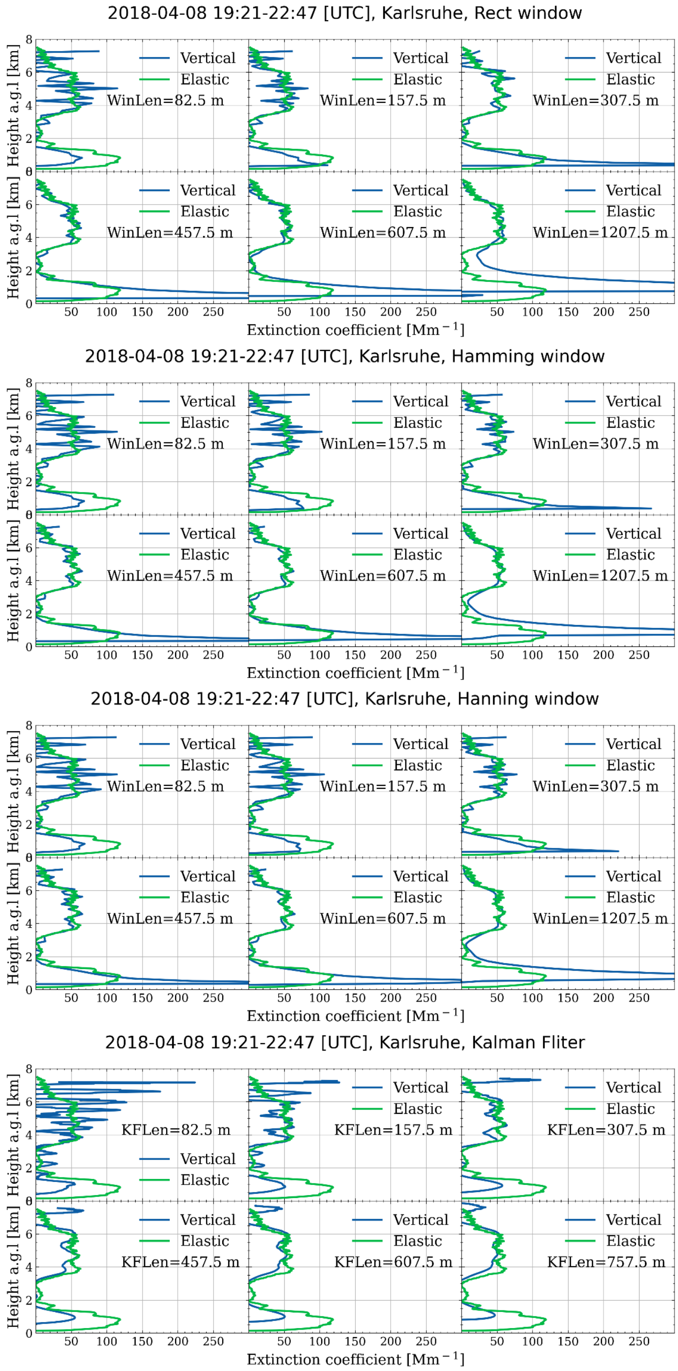

Figure S1. Extinction coefficients from Raman signal from vertical and slant measurements with different types of filters and different filter lengths.

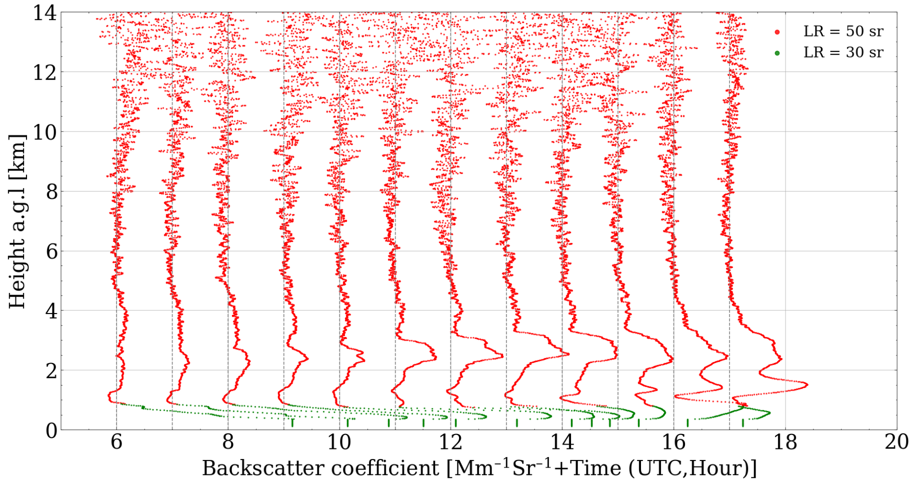

Figure S2. Elastic backscatter coefficients from vertical lidar measurement for different values of altitude-dependent lidar ratios with interval time being 1 hour on 7, April 2018.

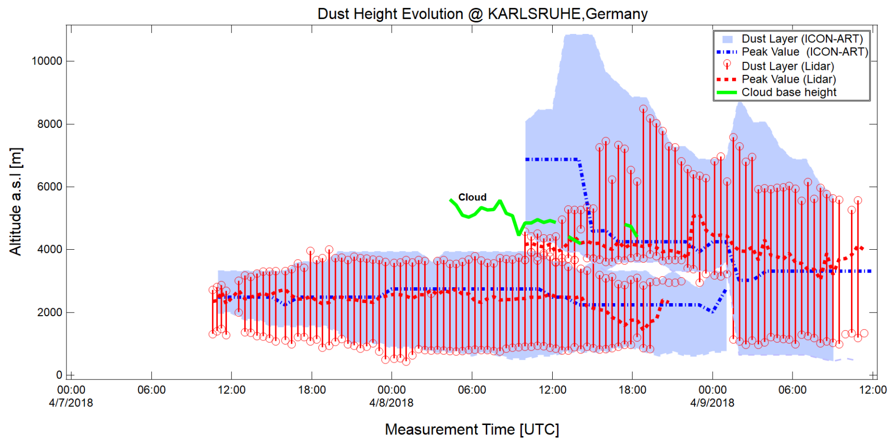

Figure S3. Time series of dust layer heights and peak heights (the heights for the maximum backscatter coefficients) for both lidar measurements and ICON-ART prediction as well as cloud base heights (green line) measured by lidar from 7 to 9, April 2018.

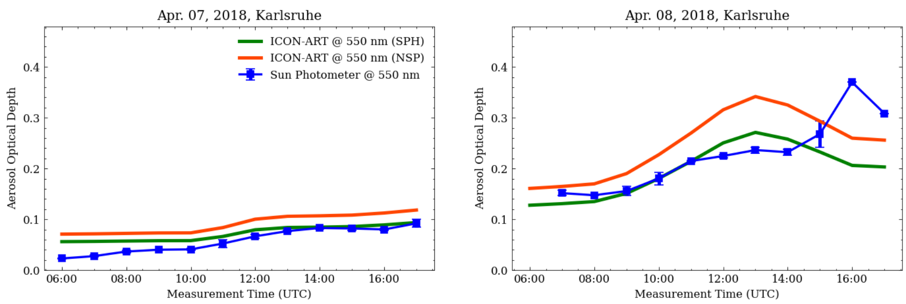

Figure S4. AOD from the sun photometer (coarse mode) and ICON-ART for both SPH and NSP particles model simulation on 7 and 8 of April for 1 hour temporal resolution. SPH = spherical; NSP = non-spherical.

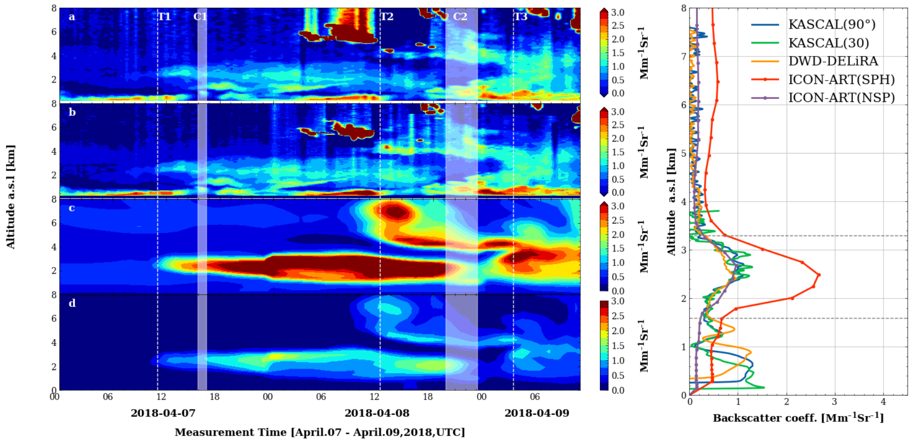

Figure S5. Time series of backscatter coefficients from KASCAL measurements (a) and from DWD-DELiRA measurements with ICON-ART results shown as black contour lines (b) as well as ICON-ART results for SPH particles (c) and as ICON-ART results for NSP particles from April 7 to 9, 2018. Please note that the model data only includes the Saharan dust while the lidar data shows also other aerosol particles and clouds. The profiles of backscatter coefficients measured by the two lidars from 15:30 to 16:30 and predicted by ICON-ART for 16:00 on April 7, 2018 (indicated as C1 in the contour plots) are shown on the right side of this figure. The vertical dashed lines in the contour plots indicate dust arrival (T1), second dust layer appeared (T2), and the two dust layers merged (T3). C1 and C2 represent time periods used for a more detailed data analysis. SPH = spherical; NSP = non-spherical.

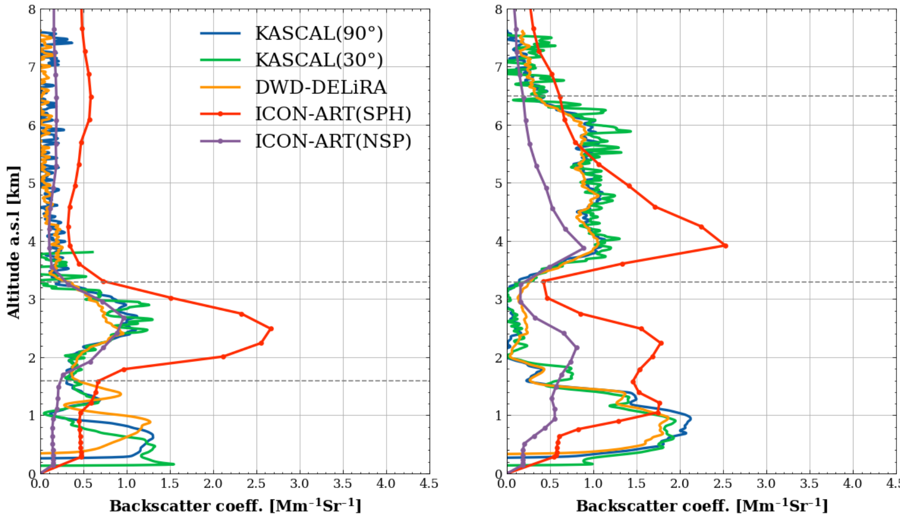

Figure S6. Profiles of backscatter coefficient from KASCAL (both vertical and slant direction), DWD-DEliRA measurements as well as ICON-ART model simulation for two typical cases indicated C1 (left) and C2 (right) in Fig.1. SPH = spherical; NSP = non-spherical.

Table S1. Averaged extinction coefficients and its their stand deviations for different window types and lengths.

Ext. coeff. (Mm^{-1})	H=82.5 m	H=157.5 m	H=307.5 m	H=457.5 m	H=607.5 m	H=1207.5 m
Rect. window	48 ± 32	49 ± 19	48 ± 11	49 ± 8	51 ± 5	53 ± 5
Hamming window	49 ± 36	48 ± 27	49 ± 14	49 ± 9	50 ± 6	51 ± 4
Hanning window	49 ± 37	48 ± 29	49 ± 16	49 ± 10	49 ± 7	51 ± 4
Kalman filter	46 ± 39	47 ± 14	46 ± 8	48 ± 8	48 ± 6	48 ± 5

Table S2. Overview of SSAs measured for Saharan dust.

SSA	Wavelength [nm]	Reference
0.88 – 0.92	439	This work
0.91	450	Müller et al., 2011
0.96 – 0.99	530	Petzold et al., 2011
0.96	537	Schladitz et al., 2009
0.96	550	Müller et al., 2011
0.98	637	Schladitz et al., 2009
0.87-0.96	675	This work
0.86-0.94	870	This work
0.98	950	Müller et al., 2011
0.85-0.94	1018	This work

Table S3. Comparsion of backscatter coefficient from lidar and ICON-ART based on spherical parameterization (SPH) and non spherical parameterization (NSP).

	Mean Mm^{-1}	Std. Mm^{-1}
DWD-DELiRA	0.72	0.36
ICON-ART (NSP)	0.71	0.37
ICON-ART (SPH)	2.15	1.14

Appendix: Mathematical derivation of Multi-angle method

The lidar equation and klett-Fernald method Can be expressed as following:

$$P(r) = C_0 T_0^2 \frac{\beta_{aer}(r) + \beta_{mol}(r)}{r^2} \exp\left(-2\int_0^r [\alpha_{aer}(r) + \alpha_{mol}(r)]dr\right) \tag{1}$$

$$\beta(r) = \frac{\mathrm{RCS}(r) * \exp\left\{2*(S_a - S_m) * \int_r^{R_{ref}} \beta_{mol}(r')dr'\right\}}{\frac{RCS(r)}{C*\beta_{\mathrm{mol}}(r_{ref})} + 2*S_a*\int_r^{R_{ref}}\left[\mathrm{RCS}(r') * \exp\left\{2*(S_a - S_m)*\int_r^{R_{ref}} \beta_{mol}(r'')dr''\right\}\right]dr'} \tag{2}$$

In term of the numerator, S_a is for the retrieval method and S_{a0} is for the input lidar ratio. Let elevation angle be θ_1 and θ_2, and $\theta_1 > \theta_2$, $\mu_1 = \frac{1}{sin\theta_1}$, $\mu_2 = \frac{1}{sin\theta_2}$, $\mu = \mu_2 - \mu_1$. For θ_1 direction:

$$P(\mu_1 r) = C_0 T_0^2 \frac{\beta_{aer}(\mu_1 r) + \beta_{mol}(\mu_1 r)}{(\mu_1 r)^2} \exp\left(-2\int_0^{\mu_1 r} [\alpha_{aer}(\mu_1 r) + \alpha_{mol}(\mu_1 r)]dr\right) \tag{3}$$

$$\beta(\mu_1 r) = \frac{\mathrm{RCS}(\mu_1 \mathrm{r}) * \exp\left\{2*(S_a - S_m)*\int_{\mu_1 r}^{\mu_1 r_{ref}} \beta_{mol}(\mu_1 r')dr'\right\}}{\frac{RCS(\mu_1 r)}{C*\beta_{mol}(\mu_1 r_{ref})} + 2*S_a*\int_{\mu_1 r}^{\mu_1 R_{ref}}\left[\mathrm{RCS}(\mu_1 r') * \exp\left\{2*(S_a - S_m)*\int_{\mu_1 r'}^{\mu_1 R'_{ref}} \beta_{mol}(\mu_1 r'')dr''\right\}\right]dr'} \tag{4}$$

For θ_2 direction:

$$P(\mu_2 r) = C_0 T_0^2 \frac{\beta_{aer}(\mu_2 r) + \beta_{mol}(\mu_2 r)}{(\mu_2 r)^2} \exp\left(-2\int_0^{\mu_2 r} [\alpha_{aer}(\mu_2 r) + \alpha_{mol}(\mu_2 r)]dr\right) \tag{5}$$

$$\beta(\mu_2 r) = \frac{\mathrm{RCS}(\mu_2 \mathrm{r}) * \exp\left\{2*(S_a - S_m)*\int_{\mu_2 r}^{\mu_2 r_{ref}} \beta_{mol}(\mu_2 r')dr'\right\}}{\frac{RCS(\mu_2 r)}{C*\beta_{\mathrm{mol}}(\mu_2 r_{\mathrm{ref}})} + 2*S_a*\int_{\mu_2 r}^{\mu_2 R_{ref}}\left[\mathrm{RCS}(\mu_2 r') * \exp\left\{2*(S_a - S_m)*\int_{\mu_2 r'}^{\mu_2 R'_{ref}} \beta_{mol}(\mu_2 r'')dr''\right\}\right]dr'} \tag{6}$$

Replace the RCS in Equation 4 and Equation 6 by Equation 3 and Equation 5, respectively. Please note that RCS = P(r)*r2. Equation (4) divided by Equation (6). For numerator:

$$\begin{aligned}
&\frac{\mathrm{RCS}(\mu_1 \mathrm{r})_1 * \exp\left\{2*(S_a - S_m)*\int_{\mu_1 r}^{\mu_1 r_{ref}} \beta_{mol}(\mu_1 r')_1 dr'\right\}}{\mathrm{RCS}(\mu_2 \mathrm{r})_2 * \exp\left\{2*(S_a - S_m)*\int_{\mu_2 r}^{\mu_2 r_{ref}} \beta_{mol}(\mu_2 r')_2 dr'\right\}} \\
&= \frac{k*[\beta_{aer}(\mu_1 r)_1 + \beta_{mol}(\mu_1 r)_1] * \exp\left(-2\int_0^{\mu_2 T}[\alpha_{aer}(\mu_1 r') + \alpha_{mol}(\mu_1 r')_1]dr'\right) * \exp\left\{2*(S_a - S_m)*\int_{\mu_1 \tau}^{\mu_1 r_{ref}} \beta_{mol}(\mu_1 r')_1 dr'\right\}}{k*[\beta_{aer}(\mu_2 r)_2 + \beta_{mol}(\mu_2 r)_2] * \exp\left(-2\int_0^{\mu_2 r}[\alpha_{aer}(\mu_2 r') + \alpha_{mol}(\mu_2 r')_2]dr'\right) * \exp\left\{2*(S_a - S_m)*\int_{\mu_2 r}^{\mu_2 r_{ref}} \beta_{mol}(\mu_2 r')_2 dr'\right\}} \\
&= \frac{\exp\left(-2\int_0^{\mu_1 r}[\alpha_{aer}(\mu_1 r') + \alpha_{mol}(\mu_1 r')_1]dr'\right) * \exp\left\{2*(S_a - S_m)*\int_{\mu_1 r}^{\mu_1 r_{ref}} \beta_{mol}(\mu_1 r')_1 dr'\right\}}{\exp\left(-2\int_0^{\mu_2 r}[\alpha_{aer}(\mu_2 r') + \alpha_{mol}(\mu_2 r')_2]dr'\right) * \exp\left\{2*(S_a - S_m)*\int_{\mu_2 r}^{\mu_2 r_{ref}} \beta_{mol}(\mu_2 r')_2 dr'\right\}} \\
&= \frac{\exp\left\{-2\int_0^{\mu_1 r_{ref}} \alpha_{mol}(\mu_1 r')_1 dr' - 2\int_0^{\mu_1 r} \alpha_{aer}(\mu_1 r')_1 dr' + 2*S_a*\int_{\mu_1 r}^{\mu_1 r_{ref}} \beta_{mol}(\mu_1 r')_1 dr'\right\}}{\exp\left\{-2\int_0^{\mu_2 r_{ref}} \alpha_{mol}(\mu_2 r')_2 dr' - 2\int_0^{\mu_2 r} \alpha_{\mathrm{aer}}(\mu_2 r')_2 dr' + 2*S_a*\int_{\mu_2 r}^{\mu_2 r_{ref}} \beta_{mol}(\mu_2 r')_2 dr'\right\}} \\
&= \frac{1}{\exp\left\{-2\int_0^{\mu r_{ref}} \alpha_{mol}(r')dr' - 2\int_0^{\mu r} \alpha_{aer}(r')dr' + 2*S_a*\int_{\mu r}^{\mu r_{ref}} \beta_{mol}(r')dr'\right\}} \\
&= \frac{1}{\exp\left\{-2\int_0^{\mu r_{ref}} \alpha_{mol}(r')dr' - 2\int_0^{\mu r} \alpha_{aer}(r')dr' + 2*S_a*\int_0^{\mu r_{ref}} \beta_{mol}(r')dr' - 2*S_a*\int_0^{\mu r} \beta_{mol}(r')dr'\right\}}
\end{aligned} \tag{7}$$

And for the denominator:

$$\frac{\frac{\mathrm{RCS}\left(\mu_1 r_{ref}\right)_1}{C*\beta_{\mathrm{mol}}\left(\mu_1 r_{ref}\right)_1}+2*\mathrm{Sa}*\int_{\mu_1 r}^{\mu_1 ref} RCS(\mu_1 r')_1 * \exp\left\{2*(S_a-S_m)*\int_{\mu_1 r}^{\mu_1 r_{ref}}\beta_{mol}(\mu_1 r'')_1 dr''\right\}dr'}{\frac{RCS\left(\mu_2 r_{ref}\right)_2}{C*\beta_{\mathrm{mol}}\left(\mu_2 r_{ref}\right)_2}+2*\mathrm{Sa}*\int_{\mu_2 r}^{\mu_2 ref} RCS(\mu_2 r')_2 * \exp\left\{2*(S_a-S_m)*\int_{\mu_2 r}^{\mu_2 r_{ref}}\beta_{mol}(\mu_2 r'')_2 dr''\right\}dr'}$$

$$=\frac{k*\exp\left(-2\int_0^{\mu_1 r_{ref}}[\alpha_{aer}(\mu_1 r)_1+\alpha_{\mathrm{mol}}(\mu_1 r)_1]dr\right)+2*S_a*\int_{\mu_1 r}^{\mu_1 ref}k*(\beta_{aer}(\mu_1 r')_1+\beta_{mol}(\mu_1 r')_1)*\exp\left(-2\int_0^{\mu_1 r_{ref}}\alpha_{mol}(\mu_1 r'')_1 dr''-2\int_0^{\mu_1 r}\alpha_{aer}(\mu_1 r'')_1 dr''+2*S_a\int_{\mu_1 r}^{\mu_1 r_{ref}}\beta_{mol}(\mu_1 r'')_1 dr''\right)}{k*\exp\left(-2\int_0^{\mu_2 r_{ref}}[\alpha_{aer}(\mu_2 r)_2+\alpha_{mol}(\mu_2 r)_2]dr\right)+2*S_a*\int_{\mu_2 r}^{\mu_2 ref}k**(\beta_{aer}(\mu_2 r')_2+\beta_{mol}(\mu_2 r')_2)*\exp\left(-2\int_0^{\mu_2 r_{ref}}\alpha_{mol}(\mu_2 r'')_2 dr''-2\int_0^{\mu_2 r}\alpha_{aer}(\mu_2 r'')_2 dr''+2*S_a\int_{\mu_2 r}^{\mu_2 r_{ref}}\beta_{mol}(\mu_2 r'')_2 dr''\right)}$$

$$=\frac{\exp\left(-2\int_0^{\mu_1 r_{ref}}[\alpha_{aer}(\mu_1 r)_1+\alpha_{mol}(\mu_1 r)_1]dr\right)+2*S_a*\int_{\mu_1 r}^{\mu_1 ref}[\beta_{aer}(\mu_1 r')_1+\beta_{mol}(\mu_1 r')_1]*\exp\left(-2\int_0^{\mu_1 r_{ref}}\alpha_{mol}(\mu_1 r'')_1 dr''-2\int_0^{\mu_1 r}\alpha_{aer}(\mu_1 r'')_1 dr''+2*S_a\int_{\mu_2 r}^{\mu_1 r_{ef}}\beta_{mol}(\mu_1 r'')_1 dr''\right)}{\exp\left(-2\int_0^{\mu_2 r_{ref}}[\alpha_{aer}(\mu_2 r)_2+\alpha_{mol}(\mu_2 r)_2]dr\right)+2*S_a*\int_{\mu_2 r}^{\mu_2 ref}[\beta_{aer}(\mu_2 r')_2+\beta_{mol}(\mu_2 r')_2]*\exp\left(-2\int_0^{\mu_2 r_{ref}}\alpha_{mol}(\mu_2 r'')_2 dr''-2\int_0^{\mu_2 r}\alpha_{aer}(\mu_2 r'')_2 dr''+2*S_a\int_{\mu_2 r}^{\mu_2 r_{ref}}\beta_{mol}(\mu_2 r'')_2 dr''\right)}$$

$$=\frac{\exp\left(-2\int_0^{\mu_1 r_{ref}}[\alpha_{aer}(\mu_1 r)_1+\alpha_{mol}(\mu_1 r)_1]dr\right)+2*S_a*\int_{\mu_1 r}^{\mu_1 ref}[\beta_{aer}(\mu_1 r')_1+\beta_{mol}(\mu_1 r')_2]*\exp\left\{-2\int_0^{\mu_1 r_{ref}}[\alpha_{mol}(\mu_1 r'')_1-S_a*\beta_{mol}(\mu_1 r'')_1]dr''-2\int_0^{\mu_1 r}[\alpha_{aer}(\mu_1 r'')_1+S_a*\beta_{mol}(\mu_1 r'')_1]dr''\right\}}{\exp\left(-2\int_0^{\mu_2 r_{ref}}[\alpha_{aer}(\mu_2 r)_2+\alpha_{mol}(\mu_2 r)_2]dr\right)+2*S_a*\int_{\mu_2 r}^{\mu_2 ref}[\beta_{aer}(\mu_2 r')_2+\beta_{mol}(\mu_2 r')_2]*\exp\left\{-2\int_0^{\mu_2 r_{ref}}[\alpha_{mol}(\mu_2 r'')_2-S_a*\beta_{mol}(\mu_2 r'')_2]dr''-2\int_0^{\mu_2 r}[\alpha_{aer}(\mu_2 r'')_2+S_a*\beta_{mol}(\mu_2 r'')_2]dr''\right\}}$$

$$=\frac{\exp\left(-2\int_0^{\mu_1 r_{ref}}[\alpha_{aer}(\mu_1 r)_1+\alpha_{mol}(\mu_1 r)_1]dr\right)+2*S_a*e^{-2\int_0^{\mu_1 r_{ref}}[\alpha_{mol}(\mu_1 r'')_1-S_a*\beta_{mol}(\mu_1 r'')_1]dr''}*\int_{\mu_1 r}^{\mu_1 ref}[\beta_{aer}(\mu_1 r')_1+\beta_{mol}(\mu_1 r')_1]*\mathrm{e}^{f(\mu_1 r)}dr}{\exp\left(-2\int_0^{\mu_2 r_{ref}}[\alpha_{aer}(\mu_2 r)_2+\alpha_{mol}(\mu_2 r)_2]dr\right)+2*S_a*e^{-2\int_0^{\mu_2 r_{ref}}[\alpha_{mol}(\mu_1 r'')_1-S_a*\beta_{mol}(\mu_2 r'')_1]dr''}*\int_{\mu_2 r}^{\mu_2 ref}[\beta_{aer}(\mu_2 r')_2+\beta_{mol}(\mu_2 r')_2]*\mathrm{e}^{f(\mu_2 r)}\mathrm{dr}} \tag{8}$$

As $\mathrm{f}'(r)=-2[S_{a_{\mathrm{in}}}*\beta_{\mathrm{aer}}(r)+S_a*\beta_{\mathrm{mol}}(r)]$. let $\mathrm{S_{ain}}=\mathrm{S_a}$, then $\mathrm{f}'^{(r)}=-2*S_a*[\beta_{aer}(r)+\beta_{mol}(r)]$

$$\int_r^{ref}B(r')*\mathrm{e}^{f(r')}dr'=\int_r^{ref}\frac{f'(r')}{-2*S_a}*\mathrm{e}^{f(r')}dr'=\int_{f(r)}^{f(ref)}\frac{1}{-2*S_a}*\mathrm{e}^{f(r')}df(r')=\frac{1}{-2*S_a}*\mathrm{e}^{f(r')}\Big|_{f(r)}^{f(r_{reff})} \tag{9}$$

$$\int_{\mu_1 r}^{\mu_1 ref}B(\mu_1 r')*\mathrm{e}^{f(\mu_1 r')}dr'=\frac{1}{-2*S_a}*\left[\mathrm{e}^{-2*S_a*\int_0^{\mu_1 r_{ref}}[\beta_{aer}(\mu_1 r')+\beta_{\mathrm{mol}}(\mu_1 r')]dr'}-\mathrm{e}^{-2*S_a*\int_0^{\mu_1 r}[\beta_{aer}(\mu_1 r')+\beta_{\mathrm{mol}}(\mu_1 r')]dr'}\right] \tag{10}$$

$$\int_{\mu\mu_2 r}^{\mu_2 ref}B(\mu_2 r')*\mathrm{e}^{f(\mu_2 r')}dr'=\frac{1}{-2*S_a}*\left[\mathrm{e}^{-2*S_a*\int_0^{\mu_2 r_{ref}}[\beta_{aer}(\mu_2 r')+\beta_{\mathrm{mol}}(\mu_2 r')]dr'}-\mathrm{e}^{-2*S_a*\int_0^{\mu_2 r}[\beta_{aer}(\mu_2 r')+\beta_{\mathrm{mol}}(\mu_2 r')]dr'}\right] \tag{11}$$

$$\begin{aligned}&\frac{\exp\left(-2\int_0^{\mu_1 r_{ref}}[\alpha_{aer}(\mu_1 r)_1+\alpha_{mol}(\mu_1 r)_1]dr\right)+2*Sa*e^{-2\int_0^{\mu_1^{1} r_{ref}}[\alpha_{mol}(\mu_1 r'')_2-S_a*\beta_{mol}(\mu_1 r'')_1]dr''}*\int_{\mu_1 r}^{\mu_1 ref}[\beta_{aer}(\mu_1 r')_1+\beta_{mol}(\mu_1 r')_1]*\mathrm{e}^{f(\mu_1 r)}dr}{\exp\left(-2\int_0^{\mu_2 r_{ref}}[\alpha_{aer}(\mu_2 r)_2+\alpha_{mol}(\mu_2 r)_2]dr\right)+2*Sa*e^{-2\int_0^{\mu_2 ref}f[\alpha_{mol}(\mu_1 r'')_1-S_a*\beta_{mot}(\mu_2 r'')_2]dr''}*\int_{\mu_2 r}^{\mu_2 ref}[\beta_{aer}(\mu_2 r')_2+\beta_{mol}(\mu_2 r')_2]*e^{f(\mu_2 r)}dr}\\&=\frac{\exp\left(-2\int_0^{\mu_1 r_{ref}}[\alpha_{aer}(\mu_1 r)_1+\alpha_{mol}(\mu_1 r)_1]dr\right)-e^{-2\int_0^{\mu_1 r_{ref}}[\alpha_{mol}(\mu_1 r'')_1-S_a*\beta_{mol}(\mu_1 r'')_1]dr''}*\mathrm{e}^{-2*S_a*\int_0^{\mu_1 r_{ref}}[\beta_{aer}(\mu_1 r')+\beta_{mol}(\mu_1 r')]dr'}-\mathrm{e}^{-2*S_a*\delta_0^{\mu_1 r}[\beta_{aer}(\mu_1 r')+\beta_{mol}(\mu_1 r')]dr'}}{\exp\left(-2\int_0^{\mu_2 r_{ref}}[\alpha_{aer}(\mu_2 r)_2+\alpha_{mol}(\mu_2 r)_2]dr\right)-e^{-2\int_0^{\mu_2 r_{ref}}\left[\alpha_{mol}(\mu_1 r'')_1-S_{a*\beta_{mol}(\mu_2 r'')_1}\right]dr''}*\mathrm{e}^{-2*S_a*\int_0^{\mu_2 r_{ref}}[\beta_{aer}(\mu_2 r')+\beta_{mol}(\mu_2 r')]dr'}-\mathrm{e}^{-2*S_a*\delta_0^{\mu_2 r}[\beta_{aer}(\mu_2 r')+\beta_{mol}(\mu_2 r')]dr'}}\\&=\frac{1}{\exp\left\{-2\int_0^{\mu r_{ref}}[S_m*\beta_{mol}(r')-S_a*\beta_{mol}(r')]dr'\right\}\exp\left\{-2*S_a*\int_0^{\mu r}[\beta_{aer}(r')+\beta_{mol}(r')]dr'\right\}}\end{aligned} \tag{12}$$

If $\mathrm{S_{ain}}=\mathrm{S_a}$, the Ratio R = 1, which means that the backscatter coefficient profiles of two elevation angle are consistent. We can also see that $\mathrm{S_{ain}}=\mathrm{S_a}$ is also the only solution for R = 1, which also means that we can indeed get the lidar ratio from this method.